Volume 7 | Number 26 | 14 July 2019 | Pages 15459–15982

# Journal of Materials Chemistry A

Materials for energy and sustainability

rsc.li/materials-a

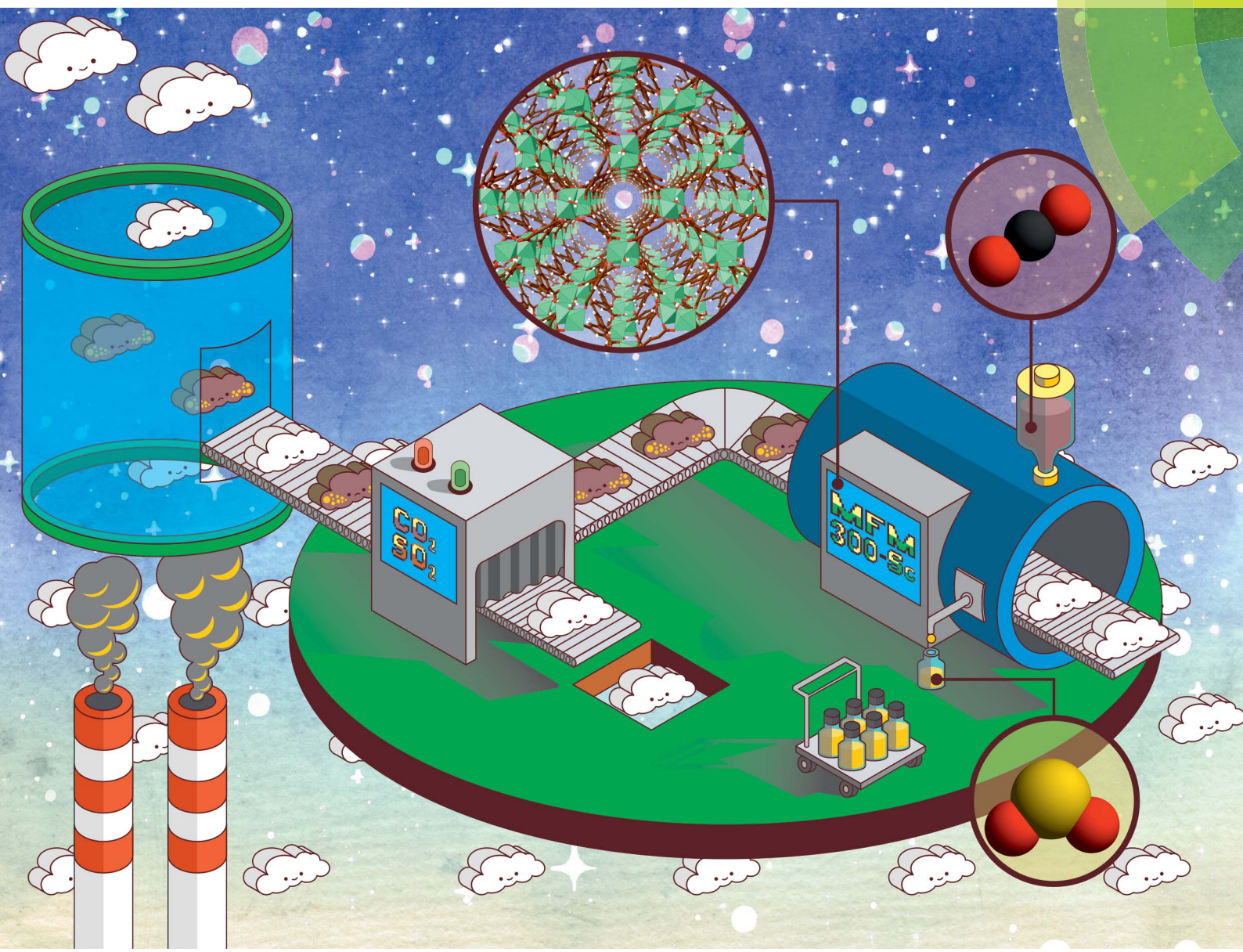


ISSN 2050-7488

ROYAL SOCIETY OF CHEMISTRY | Celebrating IYPT 2019

COMMUNICATION

Guillaume Maurin, Ilich A. Ibarra *et al.*

High and energy-efficient reversible $SO_2$ uptake by a robust Sc(III)-based MOF

Journal of Materials Chemistry A

COMMUNICATION

View Article Online
View Journal | View Issue



Cite this: J. Mater. Chem. A, 2019, 7, 15580

Received 9th March 2019
Accepted 18th April 2019

DOI: 10.1039/c9ta02585e

rsc.li/materials-a



# High and energy-efficient reversible $SO_2$ uptake by a robust Sc(III)-based MOF†

J. Antonio Zárate, ‡[ab] Elí Sánchez-González, ‡[a] Daryl R. Williams,[c] Eduardo González-Zamora,[d] Vladimir Martis,[e] Ana Martínez,[df] Jorge Balmaseda,[f] Guillaume Maurin *[b] and Ilich A. Ibarra *[a]

The MOF-type MFM-300(Sc) is demonstrated to be an optimal adsorbent for $SO_2$ capture combining high uptake, good stability and excellent cyclability involving a remarkable facile regeneration at room temperature. Interestingly, this MOF shows a drastic enhancement on its $SO_2$ uptake by 40% when a small amount of ethanol is preliminary adsorbed.

Sulphur dioxide ($SO_2$), considered as one of the most hazardous chemicals, is a colourless, non-flammable gas with a strong odour. The presence of this gas in the atmosphere is not only induced by natural events (volcanoes and wildfires) but mostly created by alarmingly increasing anthropogenic activities (fossil fuel combustion; *e.g.*, coal-fired electricity generating units).[1] This hazardous pollutant contributes to a drastic decrease of the air quality in our modern society.[2] $SO_2$ provokes severe health issues including alterations of the respiratory system (*e.g.*, broncho-constriction in lung function).[3] Typically, an exposure to only 1.5 ppm of $SO_2$ for a few minutes can cause a temporary incapability to breath normally. Moreover, this chemical is highly soluble in water and forms sulphurous acid further converted to sulfuric acid, the main component of acid rain which can damage plants, accelerate the corrosion of metals and attack limestone, marble, mortar, *etc.*[1,2] The harmful impact of this pollutant present in atmosphere is also catastrophic in terms of global warming, ozone depletion and climate change.[1–3] This dramatic situation critically urges for a significant reduction of this toxic molecule, essential to save our environment and protect billions of humans.

The current desulphurization strategy is based on the use of aqueous alkaline solutions and/or wet-sulphuric-acid processes.[4] However, these techniques produce large amounts of waste-water and traces of $SO_2$ can be left behind (approximately 400 ppm (ref. 5)), representing a major health risk according to the World Health Organization (WHO).[6] Therefore, adsorptive $SO_2$ capture strategies have been suggested as more efficient and effective alternatives.[7] The development of new and emerging sorbent materials capable to capture high amounts of $SO_2$ *via* physisorption processes is increasingly explored.[7] Although, standard porous materials such as zeolites, activated carbons and silica have been envisaged for $SO_2$ capture so far, they usually show low adsorption capacities and, in many cases, they undergo structure degradation upon $SO_2$ exposure due to the corrosive nature of this pollutant.[8]

More recently, the hybrid porous materials, namely Metal–Organic Frameworks (MOF), have been considered for $SO_2$ capture however, only a few of them proved to be stable upon $SO_2$ exposure.[9] In particular, Carson-Meredith *et al.*[10] revealed that a series of MOFs incorporating open metal sites degrade in the presence of $SO_2$. Peterson and co-workers[11] also demonstrated the decomposition of composites made of HKUST-1.

Conversely, exceptional chemically-stable MOF materials to $SO_2$ have been reported by Schröder and Yang.[12] Specifically, MFM-300(Al) (MFM = Manchester Framework Material; $[Al_2(OH)_2(L^1)]$, $L^1$ = biphenyl-3,3′5,5′-tetracarboxylate = $C_{16}O_8H_6$), an Al(III)-based MOF, previously known as NOTT-300, is a 3D open framework which comprises infinite $[AlO_4(OH)_2]$

[a]Laboratorio de Fisicoquímica y Reactividad de Superficies (LaFReS), Instituto de Investigaciones en Materiales, Universidad Nacional Autónoma de México, Circuito Exterior s/n, CU, Del. Coyoacán, 04510, Ciudad de México, Mexico. E-mail: argel@unam.mx; Tel: +52-55-5622-4595

[b]Institut Charles Gerhardt Montpellier, UMR-5253, Université de Montpellier, CNRS, ENSCM, Place E. Bataillon, 34095 Montpellier Cedex 05, France. E-mail: guillaume.maurin1@umontpellier.fr

[c]Surfaces and Particle Engineering Laboratory (SPEL), Department of Chemical Engineering, Imperial College London, South Kensington Campus, London SW7 2AZ, UK

[d]Departamento de Química, Universidad Autónoma Metropolitana-Iztapalapa, San Rafael Atlixco 186, Col. Vicentina, Iztapalapa, C. P. 09340, Ciudad de México, Mexico

[e]Surface Measurement Systems, Unit 5, Wharfside, Rosemont Road, London HA0 4PE, UK

[f]Instituto de Investigaciones en Materiales, Universidad Nacional Autónoma de México, Circuito Exterior s/n, CU, Del. Coyoacán, 04510, Ciudad de México, Mexico

† Electronic supplementary information (ESI) available: Crystal structure of MFM-300(Sc), experimental, PXRD experiments after $SO_2$, $SO_2$ adsorption experiments, Ideal Adsorbed Solution Theory (IAST) and molecular simulations. See DOI: 10.1039/c9ta02585e

‡ These authors contributed equally to this work.

octahedral chains bridged by mutually μ-OH groups, and further linked by tetradentate ligands ($L^1$).[12] This Al-MOF demonstrated a very high $SO_2$ uptake (7.1 mmol $g^{-1}$), at 298 K and 1 bar.[12] MFM-300(In), an In(III)-based MOF material isostructural to MFM-300(Al), showed an enhanced $SO_2$ uptake (8.3 mmol $g^{-1}$), at 298 K and 1 bar and a good stability towards $SO_2$ under dry and humid conditions, although no cycling experiments were reported.[13] By taking the advantage of the significant $SO_2$ adsorption properties of this robust material (MFM-300(In)), Eddaoudi and Salama fabricated an advanced chemical capacitive sensor for the detection of very low concentrations of $SO_2$ ($\approx$5 ppb) at room temperature.[14] Very recently, the Zn-based MFM-601 MOF was revealed to adsorb the highest $SO_2$ uptake (12.3 mmol $g^{-1}$) at 298 K and 1 bar, however we can emphasise that its regeneration requires relatively harsh conditions.[15]

MFM-300(Sc), formerly known as NOTT-400, was previously reported by Champness and Schröder (see Fig. S1, ESI†).[16] This Sc(III)-based MOF isostructural to MFM-300(Al) and MFM-300(In), crystallises in the chiral tetragonal space group $I4_122$ and shows a binuclear [$Sc_2$(μ-OH)] node. Each Sc(III) centre is octahedrally coordinated to six O-donors, four from different carboxylate groups of BPTC ligand (BPTC = biphenyl-3,3′,5,5′-tetracarboxylate), and two from two different μ-OH groups, see Fig. S1, ESI.† MFM-300(Sc) exhibits an overall 3D framework structure with a channel of 8.1 Å (Fig. S1, ESI†).[16] This water stable MOF MFM-300(Sc) showed interesting properties for the adsorption of diverse gases including $H_2$,[16] $CO_2$,[17] $CH_4$ (ref. 17) and vapours: $I_2$ (ref. 18) and $H_2O$.[19]

Herein, MFM-300(Sc) is demonstrated to exhibit a $SO_2$ uptake of 9.4 mmol $g^{-1}$ at 298 K and 1 bar significantly higher compared to its Al- and In-analogues, along with the retention of this level of performance after multiple $SO_2$ adsorption/desorption cycles owing to the high stability of its crystalline structure. Most importantly, the reactivation of the MFM-300(Sc) sample during the cycling experiments was performed at room temperature, that makes the adsorptive process highly energy-efficient. Advanced experimental and computational tools have been further coupled to gain insight into the molecular mechanisms responsible for the adsorption of $SO_2$ and the promising $SO_2/CO_2$ separation ability of this material. We further emphasized that a drastic $SO_2$ capture enhancement by approximately 40% is obtained when a small amount of EtOH is pre-adsorbed in MFM-300(Sc).

MFM-300(Sc) was synthesised following the previously reported recipe,[16] powder X-ray diffraction (PXRD) and thermogravimetric analysis (TGA) experiments confirmed the phase purity of the material (see Experimental details, Fig. S2 and S3, ESI†). An acetone-exchanged sample of MFM-300(Sc) was activated at 453 K and 1.7 $\times$ $10^{-3}$ Torr for 100 min and $N_2$ adsorption isotherm, at 77 K, demonstrated a BET area of approximately 1360 $m^2$ $g^{-1}$ and a total pore volume of 0.56 $cm^3$ $g^{-1}$ (see Fig. S4, ESI†) in excellent agreement with the theoretical values calculated from the crystal structure using a geometric method (1390 $m^2$ $g^{-1}$ and 0.58 $cm^3$ $g^{-1}$ respectively).

The adsorption–desorption $SO_2$ isotherm was then performed on an activated sample of MFM-300(Sc), at 298 K up to 1 bar, with the aid of a Dynamic Gravimetric Gas/Vapour Sorption Analyser, DVS vacuum (Surface Measurement Systems Ltd). The resulting adsorption isotherm is of type-I with a steep $SO_2$ uptake, from 0 to 0.05 bar, of 7.0 mmol $g^{-1}$. The isostructural MFM-300(In) was shown to exhibit a lower $SO_2$ capture of 5.9 mmol $g^{-1}$ at the same low pressure (50 mbar).[13] This MOF material, as mentioned, was used for the construction of a $SO_2$ sensor[14] in the search of practical applications where a high $SO_2$ uptake at low pressure is crucial. Thus, MFM-300(Sc) could be incorporated into a very promising, sensitive and selective $SO_2$ sensor device. From 0.05 bar to 0.2 bar the $SO_2$ uptake gradually increases to finally reach at 1 bar a value of 9.4 mmol $g^{-1}$ (see Fig. 1). We further explored the performance of the MFM-300(Al) for comparison. We evidenced that the $SO_2$ uptake at 1 bar (7.2 mmol $g^{-1}$, see Fig. S22†) remains below that recorded for the Sc-analogue. The whole $SO_2$ adsorption isotherm for MFM-300(Sc) is extremely well reproduced by the Grand Canonical Monte Carlo (GCMC) simulations. This observation emphasises that the optimal $SO_2$ adsorption performance is achieved with the consideration of our activated MFM-300(Sc). This $SO_2$ uptake is higher than that previously reported for the In-analogue which is characterised by a lower BET area and pore volume (1071 $m^2$ $g^{-1}$ and 0.42 $cm^3$ $g^{-1}$ respectively)[13] compared to MFM-300(Sc).

The isosteric heat of adsorption evaluated for $SO_2$ at low coverage (−36.2 kJ $mol^{-1}$) was found to be in very good agreement with the GCMC simulated adsorption enthalpy (−33.6 kJ $mol^{-1}$). This relatively high $SO_2$/MOF energetics is consistent with the sudden increase of the amount adsorbed at very low pressure. Analysis of the adsorption mechanism revealed that the high $SO_2$ affinity of MFM-300(Sc) comes from a strong interaction between the gas molecules *via* its O-atom and the H-atom from the μ-OH group, as illustrated by the GCMC snapshots reported in Fig. S15.†

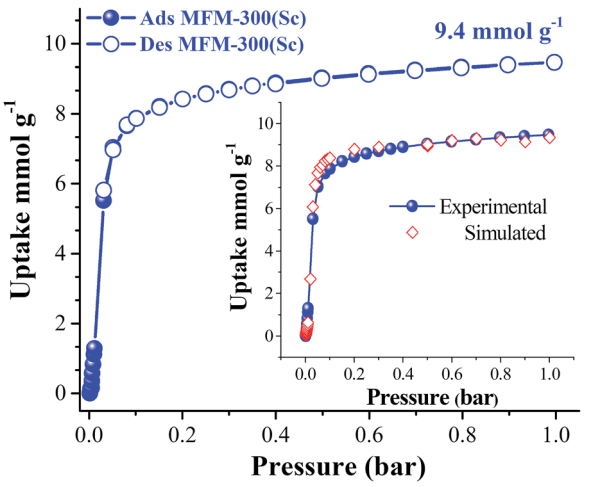


Fig. 1 Experimental $SO_2$ adsorption–desorption isotherm collected for a fully activated MFM-300(Sc) sample (filled blue circles = adsorption; open blue circles = desorption) at 298 K and up to 1 bar. The inset shows the comparison between the experimental $SO_2$ adsorption isotherm (filled blue circles) and the corresponding GCMC simulated $SO_2$ data (open red rhombus).

Cycling $SO_2$ experiments at 298 K and 1 bar were further realized in order to assess the stability of the $SO_2$ adsorption performances and the regeneration-capacity of MFM-300(Sc). Thus, after the first $SO_2$ adsorption–desorption cycle, the re-activation of this sample was conducted by only applying vacuum ($1.7 \times 10^{-6}$ Torr) for 30 minutes at 298 K. We demonstrated that the $SO_2$ adsorption capacity remains constant during 10 adsorption–desorption cycles ($9.45 \pm 0.15$ mmol $g^{-1}$, see Fig. 2). This reveals that $SO_2$ is fully released during the subsequent desorption cycles. PXRD analyses of the materials after 10 adsorption/desorption cycles confirmed the retention of the crystal structure (see Fig. S5, ESI†) while $N_2$ adsorption at 77 K evidenced that the porosity is not altered (BET area $\approx$ 1348 $m^2$ $g^{-1}$) (see Fig. S6, ESI†). This observation is a clear leap-forward for the family of MFM-300 materials since the previous studies did not report any cycling experiments for the Al- and In-analogues.[12,13] More importantly MFM-300(Sc) shows an unprecedented energy efficient and fast reactivation process, *i.e.*, room temperature treatment for 30 min under vacuum, which drastically contrasts with harsh conditions currently considered for most of the current MOFs envisaged for $SO_2$ capture.[9d,f,j,k,10] Typically, the regeneration of the best MOF reported so far, MFM-601, requires increasing the temperature to 393 K while maintaining an ultra-low pressure of $1 \times 10^{-10}$ bar for a full day.[15]

As a further stage, GCMC simulations were first employed to predict the $SO_2$ adsorption behaviour of MFM-300(Sc) in the presence of moisture (see Fig. S14†). We evidenced that the material maintains a high level of performance with a $SO_2$ uptake that only slightly decreased from 9.40 mmol $g^{-1}$ (dry conditions) to 9.16 and 9.08 mmol $g^{-1}$ under 10% and 20% of relative humidity (%RH), respectively. The separation ability of the material for the binary $SO_2/CO_2$ mixture (molar gas composition of 20 : 80 respectively) was further computationally explored. The corresponding simulated co-adsorption isotherms reported in Fig. 3 clearly highlights a much higher affinity of this MOF for $SO_2$, the corresponding $SO_2/CO_2$ selectivity attaining a value of 31 at 1 bar. This GCMC simulated separation performance was further confirmed by applying the ideal adsorbed solution theory (IAST) macroscopic model,[20] (see ESI†) to the single component adsorption isotherms which led $SO_2/CO_2$ selectivities ranging from 29 to 32 (see Fig. S12†) in the whole range of pressure and molar compositions of the gas mixture. This suggests that MFM-300(Sc) can be a promising $SO_2$ sensor as elegantly demonstrated by Salama and Eddaoudi on KAUST-7 (NbOFFIVE-1-Ni) and KAUST-8 (AlFFIVE-1-Ni) MOF materials.[21]

The GCMC simulations revealed that at low loading, $SO_2$ interacts preferentially with the μ-OH groups compared to $CO_2$ as defined by the plot of the radial distribution function for the corresponding atom pair (see Fig. S17–S20†). The presence of $CO_2$ does not significantly change the interactions between $SO_2$ and MFM-300(Sc) evidenced for the single component adsorption. An illustration of these preferential interactions and the resulting arrangements of $SO_2/CO_2$ in the pores of MFM-300(Sc) are provided in Fig. 4a and b at low and high loading, respectively. We can clearly observe that even at saturation, the large majority of $SO_2$ molecules interact with the μ-OH groups.

Finally, inspired by our previous work which demonstrated that the incorporation of polar molecules in the pores of hydroxyl (μ-OH) containing MOFs can drastically enhance their $CO_2$ capture performances,[22] we investigated the impact of pre-adsorbing a small amount of EtOH (2.6 wt%) in MFM-300(Sc) on its $SO_2$ adsorption performance at 298 K and 1 bar. Adsorption of $SO_2$ in this EtOH@MFM-300(Sc) sample showed a type-I isotherm with a sharp $SO_2$ uptake, from 0 to 0.05 bar, of 9.9 mmol $g^{-1}$ followed by a steadily increase up to reach a value of 13.2 mmol $g^{-1}$ at 1 bar (see Fig. 5) which is 40% higher compared to the value obtained for the pristine solid. When re-activating the EtOH@MFM-300(Sc) sample by applying vacuum

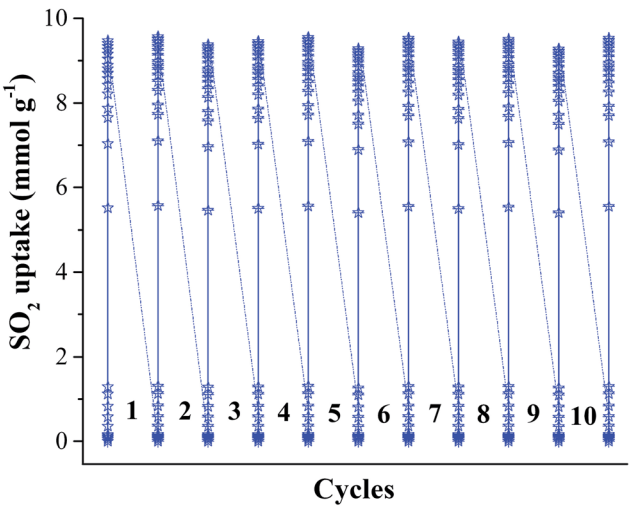


Fig. 2 Adsorption–desorption cycles for $SO_2$ in MFM-300(Sc) at 1 bar and 298 K. The re-activation of this sample was conducted by only applying vacuum ($1.7 \times 10^{-6}$ Torr) for 30 minutes at room temperature (298 K).

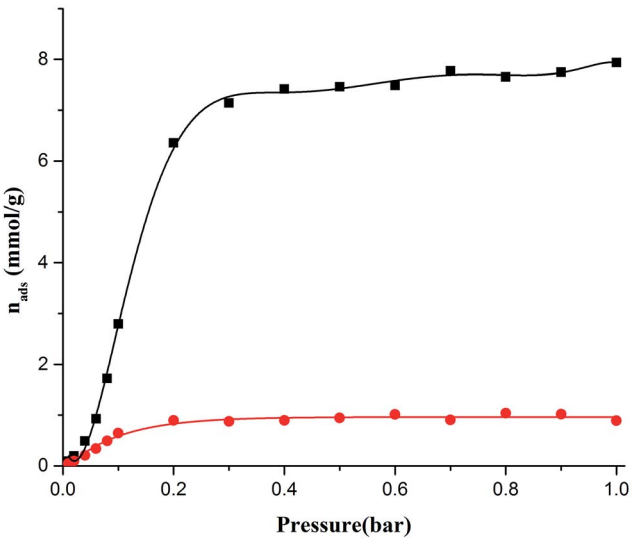


Fig. 3 GCMC simulated co-adsorption $SO_2/CO_2$ isotherms at 298 K with a molar gas composition of 20 : 80 respectively ($SO_2$: black full circle, $CO_2$: red full circle).

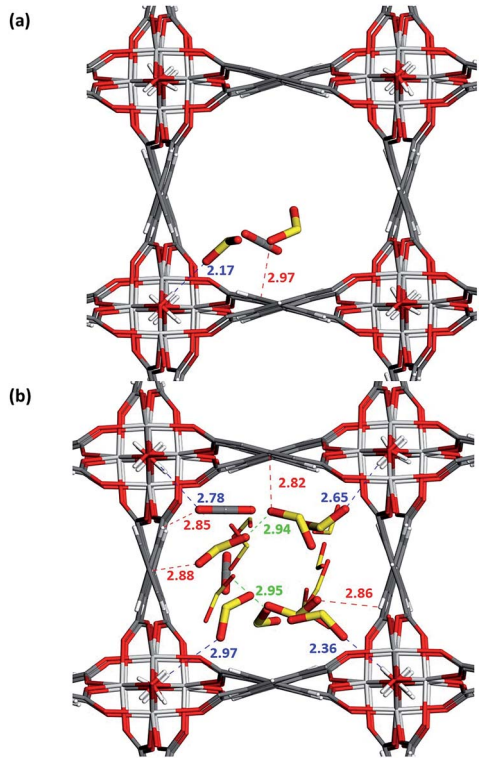


Fig. 4 (a) Illustrative arrangements of $SO_2/CO_2$ in the pores of MFM-300(Sc) generated from the GCMC simulations at 5 molecules of $SO_2$ and 1 molecule of $CO_2$ per unit cell (low loading) (b) 42.5 molecules of $SO_2$ and 5.25 molecules of $CO_2$ per unit cell (saturation capacity). The distances are reported in Å (Sc, light gray; O, red; S, yellow; C, grey; H, white). Interaction (dashes lines): $O_{SO_2}$–$H_{\mu\text{-}OH}$ (blue), $O_{SO_2}$–$H_{\mu\text{-}OH}$ (blue), $O_{SO_2}$–$C_{org}$ (red), $O_{CO_2}$–$C_{org}$ (red), $S_{SO_2}$–$C_{org}$ (red), $C_{CO_2}$–$C_{org}$ (red), $S_{SO_2}$–$O_{SO_2}$ (green), $O_{SO_2}$–$O_{SO_2}$ (green), $O_{CO_2}$–$O_{CO_2}$ (green), $C_{CO_2}$–$O_{CO_2}$ (green), $O_{SO_2}$–$O_{CO_2}$ (green), $S_{SO_2}$–$C_{CO_2}$ (green).

($1.7 \times 10^{-6}$ Torr) for 30 minutes at 298 K, the $SO_2$ adsorption capacity did not remain constant decreasing from 13.2 mmol $g^{-1}$ to 9.5 mmol $g^{-1}$ (adsorption–desorption–adsorption) and this value was essentially constant until the tenth cycle (see Fig. S24†). This result suggests that not only the $SO_2$ molecules were removed under vacuum, but also the confined EtOH molecules (2.6 wt%). Thus, a freshly synthesised EtOH@MFM-300(Sc) sample was tested for more $SO_2$ cycling experiments without the re-activation step (vacuum $1.7 \times 10^{-6}$ Torr). Then, the $SO_2$ capture was only slightly reduced in the first cycle from 13.3 mmol $g^{-1}$ to 12.9 mmol $g^{-1}$ (adsorption–desorption–adsorption, see Fig. S25†). For the second cycle, the $SO_2$ capture was reduced from 12.9 mmol $g^{-1}$ to 12.2 mmol $g^{-1}$. Finally, from this cycle to the seventh cycle, the $SO_2$ uptake went back to 9.4 mmol $g^{-1}$ and remained constant until the tenth cycle (Fig. S25†), demonstrating that EtOH molecules were "pushed out" by the $SO_2$ adsorption–desorption cycling process.

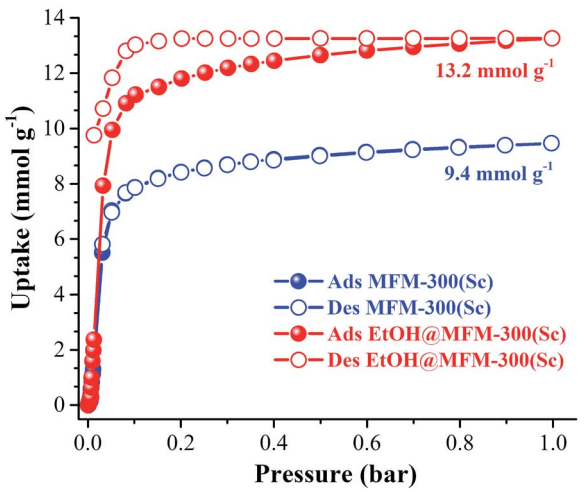


Fig. 5 $SO_2$ adsorption isotherms of MFM-300(Sc) and EtOH@MFM-300(Sc) at 298 K and 1 bar.

We also applied the same pre-adsorbing protocol (confinement of EtOH = 2.6 wt%) to MFM-300(Al), and measured the $SO_2$ uptake at 298 K and 1 bar. Thus, the EtOH@MFM-300(Al) sample showed a type-I isotherm with a total $SO_2$ uptake of 9.9 mmol $g^{-1}$ (see Fig. S23†) which is 37% higher than the amount adsorbed by the pristine MFM-300(Al). Such a strategy to enhance the $SO_2$ capture performance of a MOF has never been proposed so far. Interestingly EtOH@MFM-300(Sc) outperforms MFM-601, the current best MOF for $SO_2$ capture.[15]

To summarise, MFM-300(Sc) exhibits a high $SO_2$ uptake combined with an exceptional chemical stability towards $SO_2$, excellent cycling performances and an unprecedented facile regeneration at room temperature. Furthermore, this MOF constructed with an environmentally compatible metal centre (Sc(III)), shows a spectacular enhancement of the $SO_2$-uptake when a small amount of EtOH is pre-adsorbed, outperforming MFM-601,[15] the best $SO_2$ MOF adsorbent reported so far.

## Conflicts of interest

There are no conflicts to declare.

## Acknowledgements

The authors thank Dr A. Tejeda-Cruz (powder X-ray; IIM-UNAM) for analytical assistance. The authors thank the financial support provided by CONACyT (1789) and PAPIIT UNAM (IN101517), México. E. G.-Z. thanks CONACyT (236879), México for financial support. J. A. Z. thanks PhD CONACyT grant (577325), México. Thanks to U. Winnberg (ITAM) for scientific discussions and G. Ibarra-Winnberg for conceptualising the design of this contribution.

## Notes and references

1 J. N. Galloway, *Water, Air, Soil Pollut.*, 1995, **85**, 15.
2 M. Kampa and E. Castana, *Environ. Pollut.*, 2008, **151**, 362.
3 N. Greenberg, R. S. Carel, E. Derazne, H. Bibi, M. Shpriz, D. Tzur and B. A. Portnov, *J. Toxicol. Environ. Health, Part A*, 2016, **79**, 342.
4 P. Córdoba, *Fuel*, 2015, **144**, 274.
5 J.-Y. Lee, T. C. Keener and Y. J. Yang, *J. Air Waste Manage. Assoc.*, 2009, **59**, 725.

6 (*a*) World Health Organisation (WHO), *Air Quality Guidelines for Particulate Matter, Ozone, Nitrogen Dioxide and Sulfur Dioxide*, http://apps.who.int/iris/bitstream/10665/69477/1/WHO_SDE_PHE_OEH_06.02_eng.pdf, accessed January 2019; (*b*) J. Lelieveld, J. S. Evans, M. Fnais, D. Giannadaki and A. Pozzer, *Nature*, 2015, **525**, 367.

7 (*a*) S. Furmaniak, A. P. Terzyk, P. A. Gauden, P. Kowalczyk and G. S. Szymanski, *Chem. Phys. Lett.*, 2013, **578**, 85; (*b*) J. L. Llanos, A. E. Fertitta, E. S. Flores and E. J. Bottani, *J. Phys. Chem. B*, 2003, **107**, 8448; (*c*) P. Zhang, H. Wanko and J. Ulrich, *Chem. Eng. Technol.*, 2007, **30**, 635.

8 (*a*) F. Rezaei and C. W. Jones, *Ind. Eng. Chem. Res.*, 2013, **52**, 12192; (*b*) J. P. Boudou, M. Chehimi, E. Broniek, T. Siemieniewska and J. Bimer, *Carbon*, 2003, **41**, 1999.

9 (*a*) J. B. DeCoste and G. W. Peterson, *Chem. Rev.*, 2014, **114**, 5695; (*b*) S. Yang, J. Sun, A. J. Ramirez-Cuesta, S. K. Callear, W. I. F. David, D. P. Anderson, R. Newby, A. J. Blake, J. E. Parker, C. C. Tang and M. Schröder, *Nat. Chem.*, 2012, **4**, 887; (*c*) S. Yang, L. Liu, J. Sun, K. M. Thomas, A. J. Davies, M. W. George, A. J. Blake, A. H. Hill, A. N. Fitch, C. C. Tang and M. Schröder, *J. Am. Chem. Soc.*, 2013, **13**, 4954; (*d*) L. M. Rodriguez-Albelo, E. Lopez-Maya, S. Hamad, A. R. Ruiz-Salvador, S. Calero and J. A. R. Navarro, *Nat. Commun.*, 2017, **8**, 1; (*e*) S. Glomb, D. Woschko, G. Makhloufi and C. Janiak, *ACS Appl. Mater. Interfaces*, 2017, **9**, 37419; (*f*) K. Tan, P. Canepa, Q. Gong, J. Liu, D. H. Johnson, A. Dyevoich, P. K. Thallapally, T. Thonhauser, J. Li and Y. J. Chabal, *Chem. Mater.*, 2013, **25**, 4653; (*g*) A. S. Rad and A. Chourani, *J. Inorg. Organomet. Polym.*, 2017, **27**, 1826; (*h*) C. A. Fernandez, P. K. Thallapally, R. K. Motkuri, S. K. Nune, J. C. Sumrak, J. Tian and J. Liu, *Cryst. Growth Des.*, 2010, **10**, 1037; (*i*) P. K. Thallapally, R. K. Motkuri, C. A. Fernandez, B. P. McGrail and G. S. Behrooz, *Inorg. Chem.*, 2010, **49**, 4909; (*j*) M. Mon, E. Tiburcio, J. Ferrando-Soria, R. Gil San Millán, J. A. R. Navarro, D. Armentano and E. Pardo, *Chem. Commun.*, 2018, **54**, 9063; (*k*) X. Cui, Q. Yang, L. Yang, R. Krishna, Z. Zhang, Z. Bao, H. Wu, Q. Ren, W. Zhou, B. Chen and H. Xing, *Adv. Mater.*, 2017, **29**, 1606929.

10 S. Han, Y. Huang, T. Watanabe, S. Nair, K. S. Walton, D. S. Sholl and J. Carson Meredith, *Microporous Mesoporous Mater.*, 2013, **173**, 86.

11 G. W. Peterson, J. A. Rossin, J. B. DeCoste, K. L. Killops, M. Browe, E. Valdes and P. Jones, *Ind. Eng. Chem. Res.*, 2013, **52**, 5462.

12 S. Yang, J. Sun, A. J. Ramirez-Cuesta, S. K. Callear, W. I. F. David, D. P. Anderson, R. Newby, A. J. Blake, J. E. Parker, C. C. Tang and M. Schröder, *Nat. Chem.*, 2012, **4**, 887.

13 M. Savage, Y. Cheng, T. L. Easun, J. E. Eyley, S. P. Argent, M. R. Warren, W. Lewis, C. Murray, C. C. Tang, M. D. Frogley, G. Cinque, J. Sun, S. Rudic, R. T. Murden, M. J. Benham, A. N. Fitch, A. J. Blake, A. J. Ramirez-Cuesta, S. Yang and M. Schröder, *Adv. Mater.*, 2016, **28**, 8705.

14 V. Chernikova, O. Yassine, O. Shekhah, M. Eddaoudi and K. N. Salama, *J. Mater. Chem. A*, 2018, **6**, 5550.

15 J. H. Carter, X. Han, F. Y. Moreau, I. da Silva, A. Nevin, H. G. W. Godfrey, C. C. Tang, S. Yang and M. Schröder, *J. Am. Chem. Soc.*, 2018, **140**, 15564.

16 I. A. Ibarra, S. Yang, X. Lin, A. J. Blake, P. J. Rizkallah, H. Nowell, D. R. Allan, N. R. Champness, P. Hubberstey and M. Schröder, *Chem. Commun.*, 2011, **47**, 8304.

17 I. A. Ibarra, A. Mace, S. Yang, J. Sun, S. Lee, J.-S. Chang, A. Laaksonen, M. Schröder and X. Zou, *Inorg. Chem.*, 2016, **55**, 7219.

18 X. Zhang, I. da Silva, H. G. W. Godfrey, S. K. Callear, S. A. Sapchenko, Y. Cheng, I. Vitórica-Yrezábal, M. D. Frogley, G. Cinque, C. C. Tang, C. Giacobbe, C. Dejoie, S. Rudic, A. J. Ramirez-Cuesta, M. A. Denecke, S. Yang and M. Schröder, *J. Am. Chem. Soc.*, 2017, **139**, 16289.

19 J. R. Álvarez, R. A. Peralta, J. Balmaseda, E. González-Zamora and I. A. Ibarra, *Inorg. Chem. Front.*, 2015, **2**, 1080.

20 (*a*) A. L. Myers and J. M. Prausnitz, *AIChE J.*, 1965, **11**, 121; (*b*) C. M. Simon, B. Smit and M. Haranczyk, *Comput. Phys. Commun.*, 2016, **200**, 364.

21 M. R. Tchalala, P. M. Bhatt, K. N. Chappanda, S. R. Tavares, K. Adil, Y. Belmabkhout, A. Shkurenko, A. Cadiau, N. Heymans, G. De Weireld, G. Maurin, K. N. Salama and M. Eddaoudi, *Nat. Commun.*, 2019, **10**, 1328.

22 (*a*) E. González-Zamora and I. A. Ibarra, *Mater. Chem. Front.*, 2017, **1**, 1471; (*b*) R. A. Peralta, A. Campos-Reales-Pineda, H. Pfeiffer, J. R. Alvarez, J. A. Zárate, J. Balmaseda, E. González-Zamora, A. Martínez, D. Martínez-Otero, V. Jancik and I. A. Ibarra, *Chem. Commun.*, 2016, **52**, 10273; (*c*) E. Sánchez-González, E. González-Zamora, D. Martínez-Otero, V. Jancik and I. A. Ibarra, *Inorg. Chem.*, 2017, **56**, 5863.

 